Catena 176 (2019) 189–196

Contents lists available at ScienceDirect

Catena

journal homepage: www.elsevier.com/locate/catena

Evaluating and modelling splash detachment capacity based on laboratory experiments

Bing Wu[a], Zhanli Wang[b,c,*], Qingwei Zhang[b], Nan Shen[b], June Liu[d]

[a] Department of Civil Engineering, School of Human Settlements and Civil Engineering, Xi'an Jiaotong University, Xi'an, Shaanxi 710049, China
[b] State Key Laboratory of Soil Erosion and Dryland Farming on the Loess Plateau, Institute of Soil and Water Conservation, Northwest A&F University, Yangling, Shaanxi 712100, China
[c] State Key Laboratory of Soil Erosion and Dryland Farming on the Loess Plateau, Institute of Soil and Water Conservation, Chinese Academy of Sciences and Ministry of Water Resources, Yangling, Shaanxi 712100, China
[d] School of Geography and Tourism, Shaanxi Normal University, Xi'an, Shaanxi 710119, China

ARTICLE INFO

Keywords:
Splash detachment capacity
Rainfall intensity
Slope gradient
Rainfall kinetic energy
Flow depth

ABSTRACT

Splash erosion is recognized as an important process of water erosion on agricultural land, but evaluating and modelling splash detachment capacity on steep slopes using loessial soil were not fully studied. The objectives of this study are: (1) to evaluate the effects of slope gradient (*S*) and rainfall intensity (*I*) on splash detachment capacity (*SDr*), (2) to select the key rainfall physical parameters and hydraulic parameters affecting splash detachment capacity, (3) to establish new and more accurate experimental models between splash detachment capacity (*SDr*) and these key parameters on steep slopes for loess regions. The experiment was conducted at slopes of 12.23%, 17.63%, 26.8%, 36.4%, 40.4% and 46.63% under rainfall intensities of 48, 60, 90, 120, 138 and 150 mm h^{-1}, respectively, using simulated rainfall. Results showed that the equation between splash detachment capacity (*SDr*) with both parameters of rainfall intensity (*I*) and slope gradient (*S*) (i.e. $SDr = 0.000126 \ln(0.36S^{-0.3}I^{1.3} - 14)$) could predict *SDr* well with $R^2 = 0.85$ and Nash–Sutcliffe model efficiency (NSE) = 0.71. *SDr* was more sensitive to rainfall intensity than to slope gradient. The rainfall kinetic energy (*KE*) was the key rainfall physical parameter and the mean flow depth (*h*) was the key hydraulic parameter affecting *SDr*. The equation between *SDr* with both parameters of *KE* and h (i.e. $SDr = 0.000164 \ln(0.0031KE^{1.13}h^{-0.3} - 4.5)$) could satisfactorily predict *SDr* with $R^2 = 0.85$ and Nash–Sutcliffe model efficiency (NSE) = 0.81. The new equations (i.e. $SDr = 0.000126 \ln(0.36S^{-0.3}I^{1.3} - 14)$ and $SDr = 0.000164 \ln(0.0031KE^{1.13}h^{-0.3} - 4.5)$) could help in controlling water erosion in the loess region of China.

1. Introduction

Soil erosion is a serious ecological and environmental problem, and the main cause of land degradation and landslides in many ecosystems worldwide (Nowak and Schneider, 2017; Xu et al., 2017; Xu and Coop, 2017; Mekonnen et al., 2015; Heathcote et al., 2013; Ali et al., 2011; Karlen et al., 2003; Lal, 1998). According to Morgan (2005), soil erosion is a two-phase process that consists of the detachment of individual soil particles by raindrop and transport of these particles by sheet flow. Detachment of soil particles by splash erosion may be considered the

Abbreviations and symbols: SDr, the splash detachment capacity (kg m^{-2} s^{-1}); t_i, the sampling time (s); m_a, the weight of splash detachment by raindrops during sampling time (kg); m_d, the weight of the raindrop d (kg); m_i, the weight of sediments from runoff during sampling time (kg); *L*, the length of the test plot (m); *W*, the width of the test plot (m); *S*, the slope gradient (%); *I*, the rainfall intensity (mm h^{-1}); v_d, the fall velocity of raindrop d (m s^{-1}); v_r, the raindrop terminal velocity (m s^{-1}); V_s, the surface flow velocity (m s^{-1}); *V*, the flow velocity of sheet flow layer (m s^{-1}); V_m, the mean flow velocity of sheet flow layer (m s^{-1}); *k*, the correction coefficient; h_i, the flow depth (m); h, the mean flow depth (m); R_i, the weight of the runoff during sampling time (kg); ρ_i, the mass density of the runoff (kg m^{-3}); ρs, the mass density of the sediments (= 2650 kg m^{-3}); *P*, the water mass density (kg m^{-3}); *g*, the gravitational constant (m s^{-2}); S_i, the sine of the bed slope (m m^{-1}); *KE*, the rainfall kinetic energy (J m^{-2} h^{-1}); D_{50}, the raindrop median volume diameter (mm); *NSE*, the Nash–Sutcliffe efficiency; *RE*, the relative error; *RME*, the average absolute values of the relative error (%); R^2, the coefficient of determination; O_i, the observed values (kg m^{-2} s^{-1}); P_i, the predicted values (kg m^{-2} s^{-1}); $\overline{O}$, the mean of the observed value (kg m^{-2} s^{-1}); $\overline{P}$, the mean of the predicted value (kg m^{-2} s^{-1}); *n*, the number of samples

* Corresponding author at: State Key Laboratory of Soil Erosion and Dryland Farming on the Loess Plateau, Institute of Soil and Water Conservation, Northwest A&F University, Yangling, Shaanxi 712100, China.
E-mail address: zwang@nwsuaf.edu.cn (Z. Wang).

https://doi.org/10.1016/j.catena.2019.01.009
Received 1 May 2018; Received in revised form 21 November 2018; Accepted 8 January 2019

first step of interrill erosion by sheet flow (Fernández-Raga et al., 2017; Hu et al., 2016; Kinnell, 2005), which is affected by various factors such as rainfall intensity (Ellison, 1947; Park et al., 1983), slope gradient (Fan and Wu, 1993; Meyer and Harmon, 1989), rainfall kinetic energy (Al-Durrah and Bradford, 1981; Sharma and Gupta, 1989; Morgan et al., 1998; Hu et al., 2016), flow depth (Torri et al., 1987; Morgan et al., 1998). Thus, the accurate evaluation of splash detachment capacity in susceptible areas is necessary to the development of process-based soil erosion models, because splash erosion is the first key mechanism of the soil erosion process.

In past studies, numerous investigations have been conducted to calculate splash erosion by overland flow. The suitability of different splash erosion equations has been assessed under different experimental conditions. Ellison (1947) analysed the relationship of splash erosion with raindrop fall velocity, the raindrop volume diameter and rainfall intensity and the following equation was established:

$$D_s = 20.8KV_r^{4.33}d^{1.07}I^{0.65}, \quad (1)$$

where D_s is the weight of total splash erosion of 30 min (g), K is the soil erodible coefficient, V_r is the raindrop fall velocity (m s^{-1}), d is the raindrop volume diameter (mm), I is the rainfall intensity (mm h^{-1}). In this experiment, the raindrop diameters were 3.5 mm and 5.1 mm, and the slope gradients were 6%, 10% and 16%, and the rainfall intensities were 4.8 mm h^{-1} and 8.1 mm h^{-1}, respectively. Al-Durrah and Bradford (1981) analysed the relationship of splash erosion with rainfall kinetic energy and shear stress and the following equation was established:

$$S_p = 0.36 + 0.007KE/\tau, \quad (2)$$

where S_p is the weight of splash erosion by one raindrop (mg), KE is the rainfall kinetic energy (J), τ is the soil shear stress (kPa). In this experiment, the waterdrop diameters were 3.0, 4.6, and 5.6 mm, and the slope gradient was 0%. Sharma and Gupta (1989) analysed the relationship of splash erosion with rainfall kinetic energy and critical rainfall kinetic energy and the following equation was established:

$$D = K\ (KE - KE_0), \quad (3)$$

where D is the weight of splash erosion by raindrop (mg), K is the soil erodible coefficient, KE is the rainfall kinetic energy (mJ), KE_0 is the critical rainfall kinetic energy (mJ). In this experiment, the raindrops diameters varied from 3.6 to 5.0 mm, and the sand was used at 0% slopes. Morgan et al. (1998) analysed the relationship of splash detachment rate with the rainfall kinetic energy and the flow depth. They established an equation which was used in EUROSEM (European Soil Erosion Model), as follows:

$$DR = k\ KEe^{-zh}, \quad (4)$$

where DR is the splash detachment rate (g m^{-2} s^{-1}), k is the soil erodible coefficient, KE is the rainfall kinetic energy (J m^{-2}), z is exponent from 0.9 to 3.1, h is the flow depth (m). The influence of slope on soil particle detachment is neglected in EUROSEM. Gabet and Dunne (2003) analysed the relationship of splash detachment rate with rain power, flow depth and raindrop diameter and found that a dimensionless function, A(h, d), that accounts for the interaction of flow depths (h) and raindrop diameter (d) in moderating detachment rates. The following equation was established:

$$DR = 0.011\ R^{1.4}A(h,d), \quad (5)$$

where DR is the splash detachment rate (g m^{-2} s^{-1}), R is the rain power (W m^{-2}), h is the flow depth (cm), d is the raindrop diameter (mm). In this experiment, the slope gradients were from 6.99% to 30.56%, and the rainfall intensities were from 50 mm h^{-1} to 130 mm h^{-1}. Moreover, the median drop sizes ranged from 1.9 mm to 3.9 mm in this study. Wu and Zhou (1991) analysed the relationship of splash erosion with rainfall intensity, slope gradient and the rainfall kinetic energy and the following equation was established:

$$S_T = 5.985(KEI)^{0.544}S^{0.471}, \quad (6)$$

where S_T is the weight of splash erosion of unit area (g), KE is the rainfall kinetic energy (J m^{-2}), I is the rainfall intensity (mm min^{-1}), S is the slope gradient (°). In this experiment, the slope gradients varied from 17.62% to 57.70% and the rainfall intensities varied from 49.43 mm h^{-1} to 122.22 mm h^{-1}. Moreover, the raindrop diameters were < 4 mm. Hu et al. (2016) analysed the relationship of splash erosion with the rainfall kinetic energy and the raindrop median volume diameter and derived the following equation:

$$S_T = 0.14KE^{2.65}D_{50}{}^{0.54}, \quad (7)$$

where S_T is total splash erosion (g), KE is raindrop kinetic energy (J m^{-2} mm^{-1}), and D_{50} is the raindrop median volume diameter (mm). In this experiment, the slope gradient was 17.62% and the rainfall intensities were 50 mm h^{-1} and 100 mm h^{-1}. Moreover, the raindrop diameters varied from 2 mm to 3 mm.

Although many equations have been derived to evaluate splash erosion, Govers (1992) determined that no existing formula could perform efficiently over the entire range of available data. Dunne et al. (2010) suggested that for rain splash, developing the equation with theory and with measurements from the laboratory and the field is needed. The Loess Plateau in northwest China is characterised by steep slopes and experiences high rain intensities, and the loess soil was highly erodible. However, the existed equations were established by many researchers based on different experimental conditions such as gentle slope gradient, small rainfall intensity, different soil material and different raindrop diameters. Hence, experimental data for this region are necessary to enhance the understanding of the soil erosion process in this region. A laboratory study was conducted under controlled experimental conditions. The aims of this study was to evaluate the relationship between soil detachment capacity and slope gradient and rainfall intensity. Moreover, in order to clearly understand the dynamic mechanism of splash detachment capacity, key rainfall physical parameters and hydraulic parameters affecting splash detachment capacity were determined to establish new and more accurate experimental models between splash detachment capacity and these key parameters, as well as to verify the suitability of these models on steep slopes in the loess region of China. The results can help to deeply understand soil erosion processes.

2. Methods and materials

2.1. Experiment equipment

2.1.1. Simulated rainfall device

The experiments were conducted in the Simulation Rainfall Hall operated by the State Key Laboratory of Soil Erosion and Dryland Farming on the Loess Plateau at the Institute of Soil and Water Conservation, Chinese Academy of Sciences and the Ministry of Water Resources in Yangling, Shaanxi Province, China. A rainfall simulator system with three nozzles on two sides was used to reproduce simulated rainfall. The rainfall intensities used for this study ranged from 48 mm h^{-1} to 150 mm h^{-1}. The fall height of raindrops sprayed from the nozzles was approximately 16 m above the soil surface in all the experiments. The raindrop diameter of the simulated rainfall were from 0.125 mm to 6.0 mm, moreover, the raindrop median volume diameters were from 1.52 mm to 2.7 mm. Dispersed raindrop with different diameters were precisely created by adjusting the aperture of the nozzle orifice and the water pressure. The simulated rainfall, with uniformity higher than 90%, exhibited similar raindrop size and distribution to those of natural rainfall, which was consistent with those reported by Shen et al. (2016). The rainfall simulator system used in the study was same as that utilized in Wu et al. (2017, 2018).

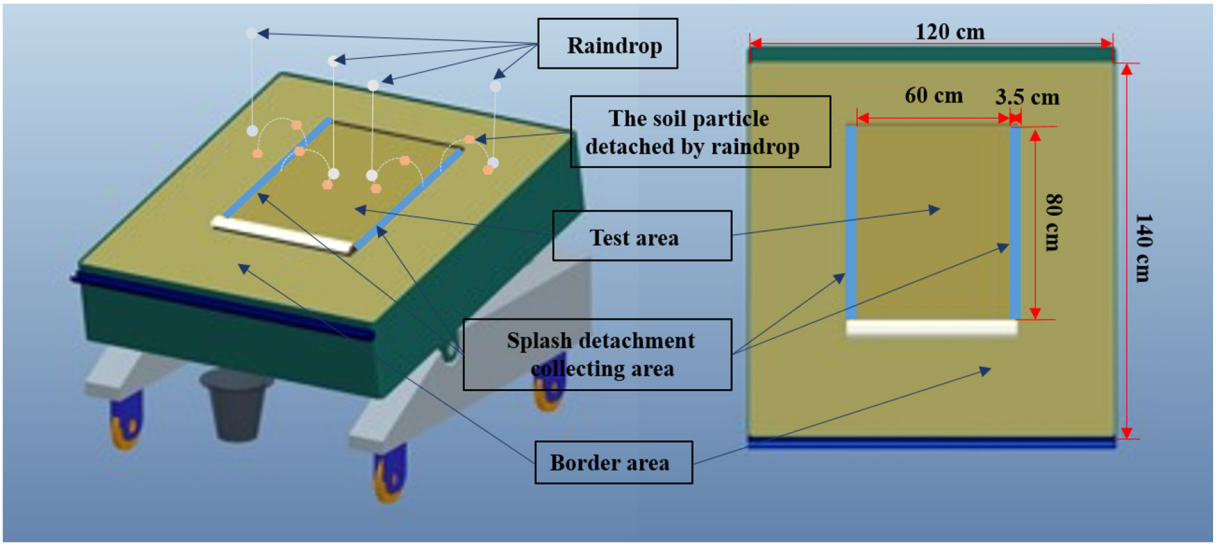

Fig. 1. The experimental device.

2.1.2. Experiment soil pan

Each experiment soil pan used in this study was modified from the soil pan designed by Meyer and Harmon (1989) and Bradford and Huang (1993). The modified pan could separately measure the splash detachment capacity on steep slopes. Each experiment soil pan with metal frames was 140 cm long, 120 cm wide and 25 cm deep. The test area was 80 cm long, 60 cm wide and 25 cm deep. The splash detachment collecting area on both sides of the test area was 80 cm long and 3.5 cm wide. A 30 cm-wide border area around the test plot was filled with soil in the same manner as the test area to equalize the opportunity for splash onto and off the area. The slope gradient for the soil pan could be adjusted between 0% and 84% (Fig. 1). The three-area soil pan used in the study was same as that utilized in Wu et al. (2018).

2.1.3. Simulated rainfall characteristic measuring device

The data of the simulated rainfall characteristics (i.e., the raindrop median volume diameter, the raindrop terminal velocity and rainfall kinetic energy) obtained by the Laser Rainfall Spectrometer (Thies Clima, Germany) (Fig. 2). The Laser Rainfall Spectrometer can measure the total number of raindrops and diameters of the raindrops and fall velocity of each raindrop per minute passing through the measurement area and the measurement area of the Laser Rainfall Spectrometer was 46.46 cm^2 (23 cm × 2.02 cm). The range of the raindrop diameters measured by the Laser Rainfall Spectrometer were from 0.16 mm to 18 mm. The range of the raindrops fall velocity measured by the Laser Rainfall Spectrometer were from 0.16 m s^{-1} to 20 m s^{-1}. The measured data were presented by chart form according to LNM-View program. The distributions of total number, diameter and fall velocity of raindrops through the measurement area in 1 min under different rainfall intensities were shown in Fig. 3.

2.2. Test soil

The test soil was collected from a depth of 0 cm to 25 cm at the farming layer of cropland. It consisted of 36.21% sand (diameter: 0.05–2.0 mm), 55.30% silt (diameter: 0.002–0.05 mm) and 8.49% clay (diameter: < 0.002 mm). Thus, the test soil was silty loam based on the soil texture classification system of United States Department of Agriculture (Huang and Zhan, 2002). The average diameter of the test soil was 0.039 mm. The test soil used in the study was same as that utilized in Wu et al. (2017, 2018).

2.3. Experiment setup

The experimental treatments used in this study included complete combination of six rainfall intensities (48, 60, 90, 120, 138 and 150 mm h^{-1}) and six slope gradients (12.23%, 17.63%, 26.8%, 36.4%, 40.40% and 46.63%), 2 replicates were undertaken.

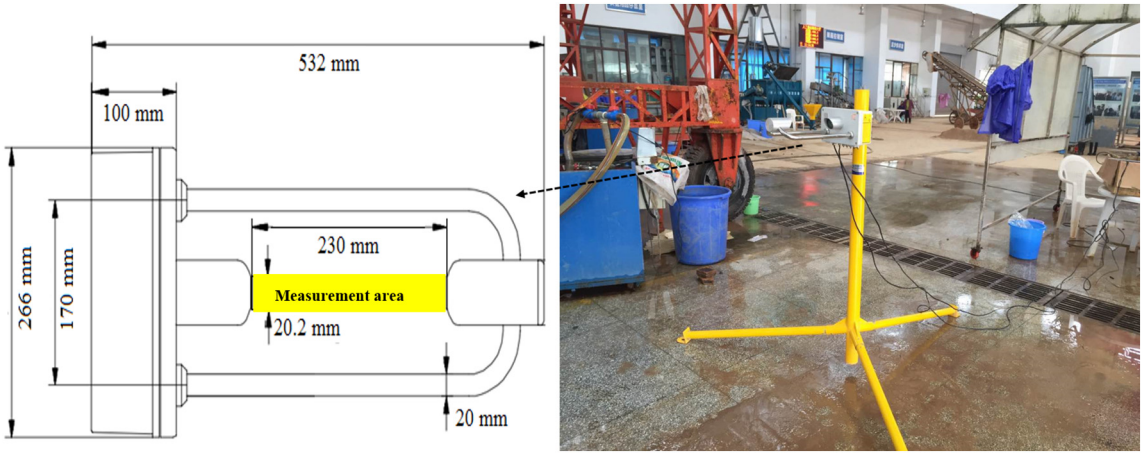

Fig. 2. The Laser Rainfall Spectrometer device.

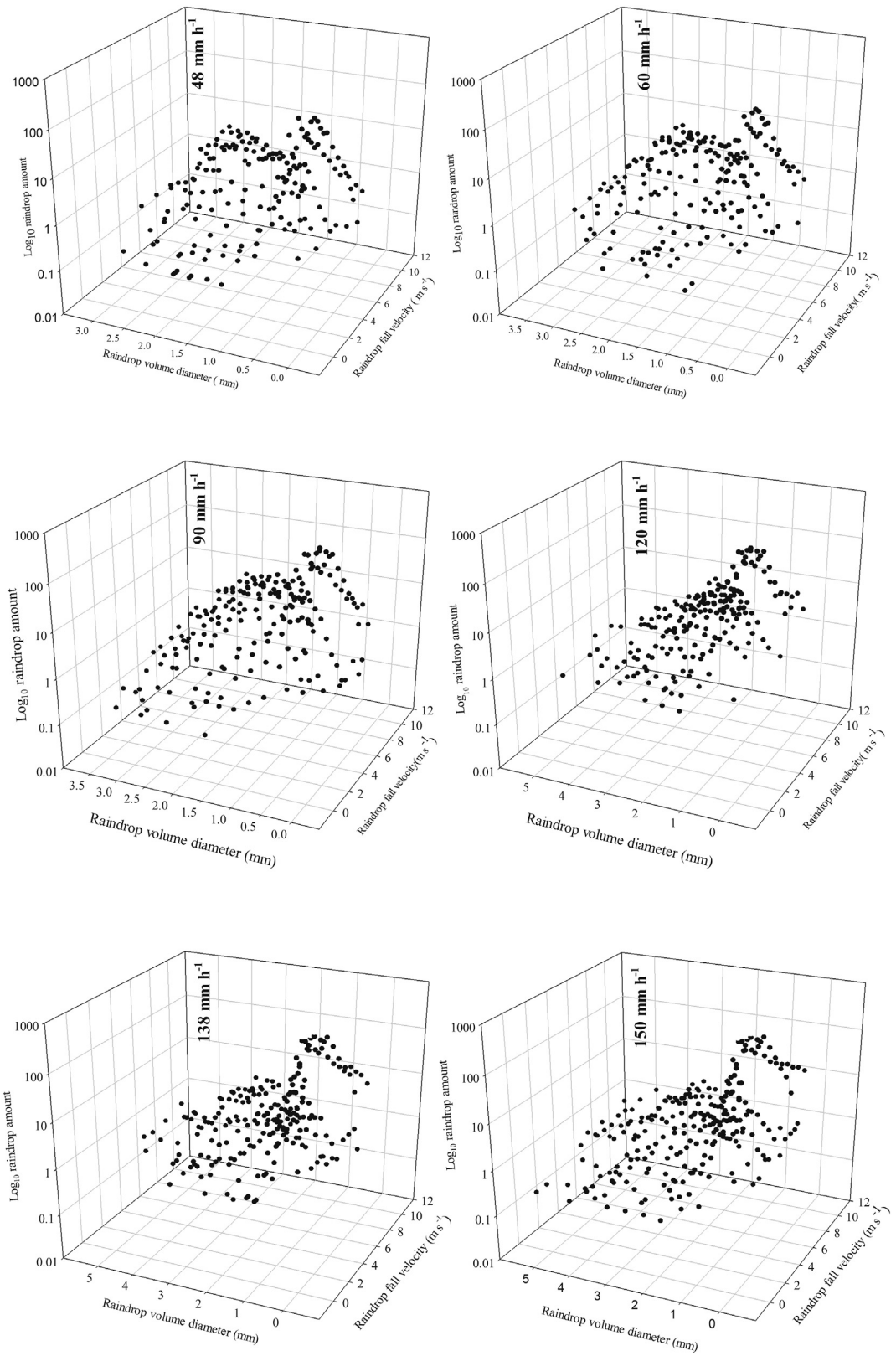

Fig. 3. Total number, diameter and velocity of raindrops falling through the test area in 1 min.

In order to assure the soil sample structure in this study is the same as which in field with similar loess soils, firstly, before packing the soil, its water content was adjusted to 14%, which was the typical level during the flood season on the Loess Plateau when most erosion would occur (Liu et al., 2014) and reflected the cohesiveness of the loess soils; secondly, A bulk density of 1.2 g cm^{-3} (measured via a cutting ring in compacted state in field with similar loess soils), which reflected the compactness of the soil, was selected for the study.

A 5 cm-thick sand layer was packed at the bottom of the soil pan, which allowed free drainage of excess water. This sand had a D_{50} value

of 0.39 mm, with 2.58% clay (< 0.002 mm), 3.94% silt (0.002–0.02 mm), fine sand 17.31% (0.02–0.2 mm) and coarse sand 76.17% (0.2–2 mm). Total porosity was 49%, and the saturated hydraulic conductivity was 5.91 mm min^{-1}. Then, the test soil was packed in the soil pan over the sand layer. The soil was packed to a depth of 20 cm. The test soil was packed in four 5 cm layers to uniformly compact the test soil. The splash detachment collecting area on both sides of the test area allowed the collection of the sediments detached by raindrops.

2.4. Experiment procedures

After preparing the soil pan, the experimental soil pan was pre-wetted with 25 mm h^{-1} rainfall intensity, which lasted for approximately 30 min. This pre-rain phase over the soil pan with a nylon net cover was designed to create uniform soil surface moisture conditions and reduce variability in soil surface micro relief which developed during the packing process, which was consistent with the method reported by An et al. (2012). Then, one day (i.e. 24 h) after the pre-rain phase, the slope gradient and rainfall intensity of the soil pan were adjusted to the levels required for this study. In the process of simulated rainfall experiment for each combination of slope gradient and rainfall intensity, samples of runoff produced by simulated rainfall were first collected for 1 min and 2 min after the onset of the runoff, and then for every 3 min until the end of the simulated rainfall experiment. For individual rainfall experiment under each combination of slope gradient and rainfall intensity, 15 runoff samples were collected. All experiments under different combination of rainfall intensities and slope gradients were undertaken two times. In addition to sampling runoff, flow velocity was measured using $KMnO_4$ as a tracer, which was easy to identify in runoff. The time during which the tracer was required to traverse a marked distance (50 cm) was determined based on the colour-front propagation using a stop watch. Surface flow velocity was measured 15 times for each treatment and the surface flow velocities were obtained from the middle of the test area each time. The splash detachment samples were weighed and left to sit to allow suspended particles to settle. The clear supernatant was decanted and the sediments left were oven-dried at 105 °C for 24 h to determine sediment weight. Splash detachment capacity was defined as splash detachment rate, which was the sediment weight of splash detachment per unit area per unit time.

2.5. Determination of date

2.5.1. Splash detachment capacity

For each combination of slope gradient and rainfall intensity, the formula that 30 splash detachment rate values were used to calculate the splash detachment capacity (SDr) of individual event is as follows:

$$SDr = \frac{1}{30}\sum_{1}^{30}\frac{m_a}{LWt_i}, \tag{8}$$

where SDr is the splash detachment capacity, which is equal to the mean splash detachment rate (kg m^{-2} s^{-1}), t_i is the sampling time (s), m_a is the sediment weight of splash detachment by raindrops during sampling time (kg), L and W are the length and the width of the test area (m).

2.5.2. Rainfall kinetic energy

For each rainfall intensity, the rainfall kinetic energy (Table 1) was calculated using the following formula:

$$KE = \sum_{1}^{n}\frac{1}{2}m_d v_d^2, \tag{9}$$

where KE is the rainfall kinetic energy (J m^{-2} h^{-1}), m_d is the weight of the raindrop d (kg), v_d is the raindrop d fall velocity (m s^{-1}).

Table 1
The raindrop kinetic energy (KE), raindrop median volume diameter (D_{50}) and raindrop terminal velocity (V_r) produced by the rainfall simulator system used in this study.

I	KE	V_r	D_{50}
mm h^{-1}	J m^{-2} h^{-1}	m s^{-1}	mm
48	201.76	1.5	1.52
60	354.85	2.7	1.6
90	495.92	3.8	1.64
120	848.82	6.5	2
138	907.63	7	2.6
150	1059.95	8.1	2.7

2.5.3. Raindrop terminal velocity

For each rainfall intensity, the raindrop terminal velocity (v_r) determined by measuring the fall velocity of raindrops (v_d) and calculated using the weighted average method (Table 1).

2.5.4. Raindrop median volume diameter

For each rainfall intensity, the raindrop median volume diameter (D_{50}) determined by corresponding to an ordinate of 50% on a cumulative volume percentage versus drop size curve (Table 1).

2.5.5. Flow velocity

The value of surface flow velocity was used to estimate the flow velocity of sheet flow layer (V) using the following formula:

$$V = kV_S, \tag{10}$$

where V_s is the surface flow velocity (m s^{-1}); V is the flow velocity of sheet flow layer (m s^{-1}) and k is the correction coefficient. The correction coefficients for the laminar, transitional and turbulent flows are 0.67, 0.7 and 0.8, respectively (Li and Abrahams, 1999; An et al., 2012). In this study, the correction coefficient was 0.67.

For each combination of slope gradient and rainfall intensity, 30 flow velocities of sheet flow layer values were used to calculate the mean flow velocity of sheet flow layer (V_m) of individual event.

2.5.6. Flow depth

The flow depth was obtained using the following formula:

$$h_i = \frac{R_i/\rho_i - m_i/\rho_s}{V_m W t_i}, \tag{11}$$

where h_i is the flow depth (m), R_i is the weight of the runoff during sampling time (i.e. t_i) (kg), ρ_i is the mass density of the runoff (kg m^{-3}), ρ_s is the mass density of the sediments (2650 kg m^{-3}), m_i is the weight of sediments from runoff during sampling time (kg), V_m is the mean flow velocity of the sheet flow layer (m s^{-1}) and t_i is the sampling time (s).

For each combination of slope gradient and rainfall intensity, thirty flow depth values were used to calculate the mean flow depth (h).

2.6. Data analysis

The data set was adopted to derive new equations that could describe the relationship of splash detachment capacity with rainfall intensity, slope gradient, rainfall characteristic and the hydraulic parameters via regression analysis, as well as to derive the values of the statistical parameters R^2, RE, RME and NSE, which were used to evaluate the performance of new equations. The values of R^2, RE, RME and NSE were calculated as follows:

$$RE = \frac{(O_i - P_i)}{O_i} \times 100, \tag{12}$$

$$RME = \frac{1}{n}\sum_{i=1}^{n}\left|\frac{(O_i - P_i)}{O_i}\right| \times 100\%, \quad (13)$$

$$R^2 = \frac{[\sum_{i=1}^{n}(O_i - \overline{O})(P_i - \overline{P})]^2}{\sum_{i=1}^{n}(O_i - \overline{O})^2 \sum_{i=1}^{n}(P_i - \overline{P})^2}, \quad (14)$$

$$NSE = 1 - \frac{\sum (O_i - P_i)^2}{\sum (O_i - \overline{O})^2}, \quad (15)$$

where RE is the relative error, RME is the average absolute values of the relative error, R^2 is the coefficient of determination, O_i are the observed values, P_i are the predicted values, $\overline{O}$ is the mean of the observed value, $\overline{P}$ is the mean of the predicted value and NSE is the Nash–Sutcliffe model efficiency (Nash and Sutcliffe, 1970). NSE is a normalised statistic that reflects the relative magnitude of the residual variance compared with the variance of the observed data [good (NSE > 0.7), satisfactory (0.4 < NSE ≤ 0.7) and unsatisfactory (NSE ≤ 0.4)] (Moriasi et al., 2007; Ahmad et al., 2011; An et al., 2012). A correlation matrix of the Pearson correlation coefficient was used to analyse the correlations between splash detachment capacity with rainfall physical parameters and hydraulic parameters using SPSS 16.0 software (SPSS Inc.)

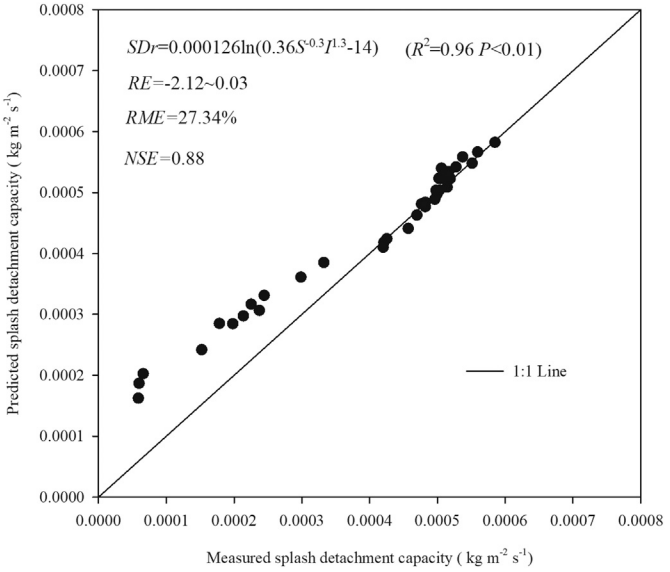

Fig. 5. Measured vs. predicted SDr (using Eq. (16)).

3. Results

3.1. Splash detachment capacity estimated using slope gradient and rainfall intensity

Fig. 4 shows that splash detachment capacity changes with different slope gradients and rainfall intensities. Evidently, splash detachment capacity was strongly influenced by slope gradient and rainfall intensity. Splash detachment capacity increased as the rainfall intensities increased, but splash detachment capacity decreased as the slope gradients increased.

For the same slope gradient level, splash detachment capacity obviously increased when rainfall intensities changed from 48 mm h^{-1} to 90 mm h^{-1}, however, the influence of slope gradient on splash detachment capacity was weakened.

To evaluate the relationship of splash detachment capacity with slope gradient and rainfall intensity, multivariate regression analyses were conducted to obtain the following relationship using the data set:

$$SDr = 0.000126\ln(0.36S^{-0.3}I^{1.3} - 14)\ (R^2 = 0.96, NSE = 0.88, P < 0.01, n = 36); \quad (16)$$

where *SDr* is the splash detachment capacity (kg m^{-2} s^{-1}), *S* is the slope gradient (%), *I* is the rainfall intensity (mm h^{-1}) and *n* is the number of samples. Logarithmic relationship exists between splash detachment capacity and slope gradient and rainfall intensity. Apparently, R^2 revealed that *SDr* was highly correlated with S and I with $R^2 = 0.96$ and this relationship of *SDr*, *S* and *I* is highly significant with $P < 0.01$; *NSE* revealed the relative magnitude of the residual variance compared with the variance of the observed data and Eq. (16) was good to predict *SDr* with *NSE* = 0.88. Overall, Eq. (16) could be used to predict *SDr* with $R^2 = 0.96$ and *NSE* = 0.88. However, the predicted splash detachment capacities were slightly greatly than the measured values when the measured splash detachment capacities < 0.0003 kg m^{-2} s^{-1}, and the predicted splash detachment capacities were very close to the measured values when the measured splash detachment capacity > 0.0003 kg m^{-2} s^{-1}(Fig. 5). The exponents of slope gradient and rainfall intensity were −0.3 and 1.3, respectively, and the exponent of slope gradient was lower than that of rainfall intensity. Thus, *SDr* was more sensitive to rainfall intensity than to slope gradient.

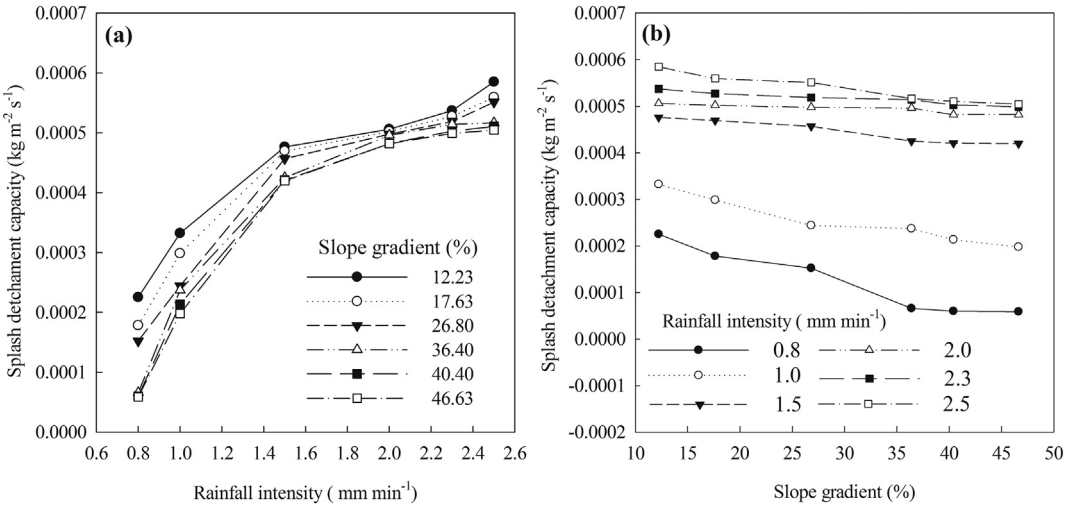

Fig. 4. SDr changed with slope gradient and rainfall intensity.

Table 2
Correlation matrix ($n = 36$) for splash detachment capacity (SDr) and the rainfall physical parameters of raindrop kinetic energy (KE), raindrop median volume diameter (D_{50}), and raindrop terminal velocity (V_r) and the hydraulic parameters of the mean flow velocity of sheet flow layer (V_m) and the mean flow depth (h).

Parameter	SDR	KE	D_{50}	V_r	V_m	h
SDR	1					
KE	0.899**	1				
D_{50}	0.756**	0.928**	1			
V_r	0.897**	1.000**	0.928**	1		
V_m	0.366*	0.565**	0.519**	0.565**	1	
h	0.468**	0.636**	0.590**	0.636**	0.911**	1

** $P < 0.01$.
* $P < 0.05$.

3.2. Correlations between splash detachment capacity with rainfall physical and hydraulic parameters

A correlation matrix of the Pearson correlation coefficient was used to analyse the correlations between splash detachment capacities with each rainfall physical and hydraulic parameter (Table 2). The rainfall kinetic energy (*KE*), the raindrop median volume diameter (D_{50}), the raindrop terminal velocity (*Vr*), the mean flow velocity of sheet flow (V_m), the mean flow depth (*h*) were taken into account. The correlations between splash detachment capacities with rainfall physical parameters decreased as follows:

$KE > V_r > D_{50}$, and the correlations between splash detachment capacity with hydraulic parameters decreased as follows: $h > V_m$. Thus, based on the correlation matrix, *KE* were the key rainfall physical parameter for evaluating splash detachment capacity and *h* was the key hydraulic parameter for evaluating splash detachment capacity.

3.3. Equation fitting between splash detachment capacity with KE and h

To evaluate the relationship of splash detachment capacity with rainfall kinetic energy (*KE*) and the mean flow depth (*h*), multivariate regression analyses were conducted to obtain the following relationship using the data set:

$$SDr = 0.000164 \ln(0.0031 KE^{1.13} h^{-0.3} - 4.5) \; (R^2 = 0.97, NSE = 0.94, P < 0.01, n = 36); \quad (17)$$

where *SDr* is the splash detachment capacity ($kg\,m^{-2}\,s^{-1}$), *KE* is the rainfall kinetic energy ($J\,m^{-2}\,h^{-1}$), *h* is the mean flow depth (m) and *n* is the number of samples. Logarithmic relationship exists between splash detachment capacity and rainfall kinetic energy and the mean flow depth. Apparently, R^2 revealed that *SDr* was highly correlated with *KE* and *h* with $R^2 = 0.97$ and this relationship of *SDr*, *KE* and *h* is highly significant with $P < 0.01$; *NSE* revealed the relative magnitude of the residual variance compared with the variance of the observed data and Eq. (17) was good to predict *SDr* with *NSE* = 0.94, respectively, The observed and simulated values of splash detachment capacity were in close agreement (Fig. 6). Hence, Eq. (17) could be used to predict *SDr* well with $R^2 = 0.97$ and *NSE* = 0.94. The exponents of rainfall kinetic energy and the mean flow depth were 1.13 and-0.3, respectively. First, the exponent of the mean flow depth was lower than that of rainfall kinetic energy. Thus, *SDr* was more sensitive to rainfall kinetic energy than to the mean flow depth. Second, the rainfall kinetic energy have a positive impact on splash detachment capacity, contrary to the negative impact of splash detachment capacity.

4. Discussion

In this study, rainfall intensity and slope gradient significantly influence splash detachment capacity. In addition, a logarithmic function

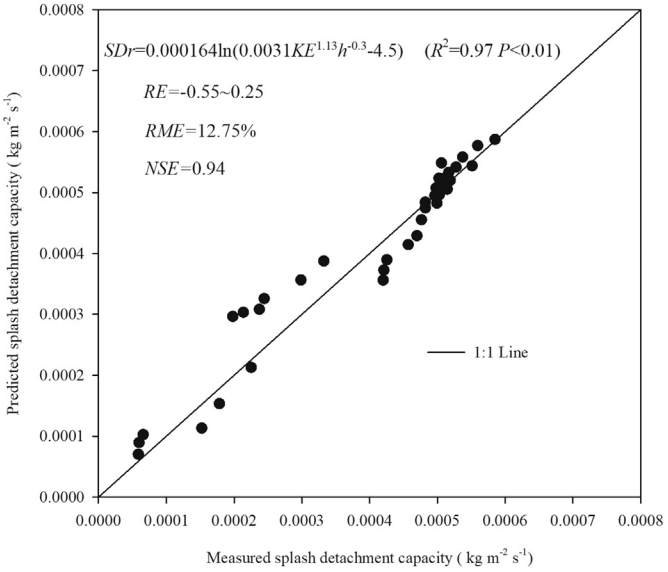

Fig. 6. Measured vs. predicted SDr (using Eq. (17)).

of rainfall intensity and slope gradient can be used to predict splash detachment capacity well. This new founding is not consistent with previous reports (Ellison, 1947; Park et al., 1983; Wu and Zhou, 1991), which suggested that splash detachment capacity could be predicted by a power function of rainfall intensity and slope gradient. In addition, Fan and Wu (1993) suggested that linear functions that existed between splash detachment capacity and rainfall intensity. In this study, the exponent of slope gradient (−0.3) revealed that the slope gradient have negative impact on splash detachment capacity, and this result is contrary to the reports by Wu and Zhou (1991) and Fan and Wu (1993). By contrast, the exponent of rainfall intensity (1.3) revealed that rainfall intensity has positive impact on splash detachment capacity, and this result is consistent with previous reports (Ellison, 1947; Park et al., 1983; Wu and Zhou, 1991).

In this study, we found that *KE* was the key rainfall physical parameter for evaluating splash detachment capacity, this result is consistent with many previous reports (Al-Durrah and Bradford, 1981; Sharma and Gupta, 1989; Wu and Zhou, 1991; Fan and Wu, 1993; Morgan et al., 1998; Van Dijk et al., 2002; Rouhipour et al., 2006; Hu et al., 2016). Thus, the rainfall kinetic energy is a sensitive parameter to splash detachment capacity. In addition, *h* was the key hydraulic parameter for evaluating splash detachment capacity, and this result is consistent with the result by Morgan et al. (1998).

A new equation of Eq. (17) was derived to predict splash detachment capacity using the rainfall kinetic energy and the mean flow depth and Eq. (17) could be used to satisfactorily predict splash detachment capacity. Eq. (17) revealed that a logarithmic function existed between the splash detachment capacity and the rainfall kinetic energy, this result is inconsistent with the reports by Morgan et al. (1998) and Hu et al. (2016), who found that a power function existed between splash detachment capacity and the rainfall kinetic energy. Eq. (17) also revealed that the flow depth has negative impact on splash detachment capacity, this result is consistent with the reports by Morgan et al. (1998) and Torri et al. (1987). Thus, this result show that the splash detachment capacity decreases as the runoff depth increases, indicating that the detachment power of the raindrops is partially dispersed by the sheet flow layer.

5. Conclusion

In this study, the relationship of splash detachment capacity with rainfall intensity, slope gradient, rainfall physical parameters (i.e., the

rainfall kinetic energy, the raindrop median volume diameter, the raindrop fall velocity and hydraulic parameters) (i.e., the mean flow velocity of sheet flow, the mean flow depth) was investigated using simulated rainfall. The results of this study demonstrated that the splash detachment capacity was increased as the rainfall intensities increased, but decreased as the slope gradients increased. Splash detachment capacity was more sensitive to rainfall intensity than to slope gradient. Eq. (16) could be used to satisfactorily predict *SDr* with $R^2 = 0.96$ and $NSE = 0.88$. In addition, *KE* was the key rainfall physical parameter for evaluating splash detachment capacity and *h* was the key hydraulic parameter for evaluating splash detachment capacity depending on the correlation matrix. Eq. (17) could be used to predict *SDR* well with $R^2 = 0.97$ and $NSE = 0.94$. *SDr* was more sensitive to rainfall kinetic energy than to the mean flow depth. The rainfall kinetic energy showed a positive impact on splash detachment capacity, however, the mean flow depth has a negative impact on splash detachment capacity.

Overall, the proposed model can facilitate the prediction of the splash detachment capacity under our study conditions and can be used to integrate processes-based soil erosion model in field, which can be used to predict soil erosion intensity in field. However, these models should be used judiciously. Additional studies are needed to develop equations/models that can optimize the processes-based soil erosion model in the Loess Plateau.

Acknowledgments

Financial support for this research was provided by the National Natural Science Foundation of China funded project (41471230; 41830758; 41601282; 41171227); the National Key Research and Development Program of China (2016YFC0402401; 2017YFD0800502); Special-Funds of Scientific Research Programs of State Key Laboratory of Soil Erosion and Dryland Farming on the Loess Plateau (A314021403-C2).

References

Ahmad, H.M.N., Sinclair, A., Jamieson, R., Madani, A., Hebb, B., Havard, P., Yiridoe, E.K., 2011. Modeling sediment and nitrogen export from a rural watershed in Eastern Canada using the soil and water assessment tool. J. Environ. Qual. 40, 1182–1194.
Al-Durrah, M., Bradford, J.M., 1981. New methods of studying soil detachment due to waterdrop impact. Soil Sci. Soc. Am. J. 45 (5), 949–953.
Ali, M., Sterk, G., Seeger, M., et al., 2011. Effect of hydraulic parameters on sediment transport capacity in overland flow over erodible beds. Hydrol. Earth Syst. Sci. Discuss. 8 (4), 6939–6965.
An, J., Zheng, F., Lu, J., Li, G., 2012. Investigating the role of raindrop impact on hydrodynamic mechanism of soil erosion under simulated rainfall conditions. Soil Sci. 177 (8), 517–526.
Bradford, J.M., Huang, C.H., 1993. Comparison of interrill soil loss for laboratory and feld procedures. Soil Technol. 6, 145–156.
Dunne, T., Malmon, D.V., Mudd, S.M., 2010. A rain splash transport equation assimilating field and laboratory measurements. Journal of Geophysical Research: Earth Surface 115, 1–16 (F01001).
Ellison, W.D., 1947. Soil erosion study-part V: soil transport in the splash process. Agric. Eng. 28, 349–351,353.
Fan, R.S., Wu, P.T., 1993. Splash erosion and sediment transport model on hillslope. J. Hydraul. Eng. 6, 24–29 (in Chinese).
Fernández-Raga, M., Palencia, C., Keesstra, S., Jordán, A., Fraile, R., Angulo-Martínez, M., Cerdà, A., 2017. Splash erosion: a review with unanswered questions. Earth Sci. Rev. 171.
Gabet, E.J., Dunne, T., 2003. Sediment detachment by rain power. Water Resour. Res. 39 (1), ESG1-1–ESG1-12.
Govers, G., 1992. Evaluation of transporting capacity formulae for overland flow. In: Parsons, A.J., Abrahams, A.D. (Eds.), Overland Flow Hydraulics and Erosion Mechanics. University College London Press, London, pp. 243–273.
Heathcote, A.J., Filstrup, C.T., Downing, J.A., 2013. Watershed sediment losses to lakes accelerating despite agricultural soil conservation efforts. PLoS One 8 (1), e53554.
Hu, W., Zheng, F.L., Bian, F., 2016. The directional components of splash erosion at different raindrop kinetic energy in the Chinese Mollisol Region. Soil Sci. Soc. Am. J. 80 (5), 1329–1340.
Huang, G.H., Zhan, W.H., 2002. Fractal property of soil particle size distribution and its application. Acta Pedol. Sin. 39 (4), 490–497 (in Chinese).
Karlen, D.L., Andrews, S.S., Weinhold, B.J., Doran, J.W., 2003. Soil quality: humankind's foundation for survival. J. Soil Water Conserv. 58, 171–179.
Kinnell, P.I.A., 2005. Raindrop-impact-induced erosion processes and prediction: a review. Hydrol. Process. 19, 2815–2844.
Lal, R., 1998. Soil erosion impact on agronomic productivity and environment quality. Crit. Rev. Plant Sci. 17 (4), 319–464.
Li, G., Abrahams, A.D., 1999. Controls of sediment transport capacity in laminar interrill flow on stone-covered surfaces. Water Resour. Res. 35 (1), 305–310.
Liu, J.E., Wang, Z.L., Yang, X.M., Jiao, N., Shen, N., Ji, P.F., 2014. The impact of natural polymer derivatives on sheet erosion on experimental loess hillslope. Soil Tillage Res. 139, 23–27.
Mekonnen, M., Keesstra, S., Stroosnijder, L., Baartman, J., Maroulis, J., 2015. Soil conservation through sediment trapping: a review. Land Degrad. Dev. 26, 544–556.
Meyer, L.D., Harmon, W.C., 1989. How row-sideslope length and steepness affect sideslope erosion. Trans. ASAE 32, 639–644.
Morgan, R.P.C., 2005. Soil Erosion and Conservation. Blackwell Publishing, Oxford.
Morgan, R.P.C., Quinton, J.N., Smith, R.E., Govers, G., Poesen, J.W.A., Auerswald, K., Styczen, M.E., 1998. The European soil erosion model (EUROSEM): a dynamic approach for predicting sediment transport from fields and small catchments. Earth Surf. Proc. Land. 23 (6), 527–544.
Moriasi, D.N., Arnold, J.G., Van Liew, M.W., Bingner, R.L., Harmel, R.D., Veith, T.L., 2007. Model evaluation guidelines for systematic quantification of accuracy in watershed simulations. Trans. ASABE 50 (3), 885–900.
Nash, J., Sutcliffe, J.V., 1970. River flow forecasting through conceptual models part I-a discussion of principles. J. Hydrol. 10 (3), 282–290.
Nowak, A., Schneider, C., 2017. Environmental characteristics, agricultural land use, and vulnerability to degradation in Malopolska Province (Poland). Sci. Total Environ. 590–591, 620–632.
Park, S.W., Mitchell, J.K., Bubenzern, G.D., 1983. Rainfall characteristics and their relation to splash erosion. Trans. ASAE 26 (3), 795–804.
Rouhipour, H., Ghadiri, H., Rose, C.W., 2006. Investigation of the interaction between flow-driven and rainfall-driven erosion processes. Soil Res. 44, 503–514.
Sharma, P.P., Gupta, S.C., 1989. Sand detachment by single raindrops of varying kinetic energy and momentum. Soil Sci. Soc. Am. J. 53 (4), 1005–1010.
Shen, H., Zheng, F., Wen, L., Han, Y., Hu, W., 2016. Impacts of rainfall intensity and slope gradient on rill erosion processes at loessial hillslope. Soil Till. Res. 155, 429–436.
Torri, D., Sfalanga, M., Del Sette, M., 1987. Splash detachment: runoff depth and soil cohesion. Catena 14 (1–3), 149–155.
Van Dijk, A.I.J.M., Bruijnzeel, L.A., Rosewell, C.J., 2002. Rainfall intensity-kinetic energy relationships: a critical literature appraisal. J. Hydrol. 261 (1–4), 1–23.
Wu, P.T., Zhou, P.H., 1991. The impact of surface slope on raindrop splash erosion. Bull. Soil Water Conserv. 11 (3), 8–13 28. (In Chinese).
Wu, B., Wang, Z., Zhang, Q., Shen, N., Liu, J., 2017. Modelling sheet erosion on steep slopes in the loess region of China. J. Hydrol. 553, 549–558.
Wu, B., Wang, Z., Zhang, Q., Shen, N., 2018. Distinguishing transport-limited and detachment-limited processes of interrill erosion on steep slopes in the Chinese loessial region. Soil Tillage Res. 177, 88–96.
Xu, L., Coop, M.R., 2017. The mechanics of a saturated silty loess with a transitional mode. Géotechnique 67 (7), 581–596.
Xu, L., Coop, M.R., Zhang, M., Wang, G., 2017. The mechanics of a saturated silty loess and implications for landslides. Eng. Geol. 236.